STUK-A125 OCTOBER 1995

Transport of Large Particles Released in a Nuclear Accident

R. Pöllänen, H. Toivonen, J. Lahtinen, T. Ilander

FINNISH CENTRE FOR RADIATION
AND NUCLEAR SAFETY
P.O.BOX 14 FIN-00881 HELSINKI
Finland
Tel. +358 0 759881

ISBN 951-712-068-0
ISSN 0781-1705

Painatuskeskus Oy
Helsinki 1995

Sold by:
Finnish Centre for Radiation and Nuclear Safety
P.O. Box 14 FIN-00881 Helsinki
Tel. +358 0 759881

PÖLLÄNEN R, TOIVONEN H, LAHTINEN J, ILANDER T. Transport of Large Particles Released in a Nuclear Accident. Helsinki 1995, 39 pp.

ISBN 951-712-068-0
ISSN 0781-1705
Key words Radioactive particles, nuclear reactor accident, particle transport

ABSTRACT

Highly radioactive particulate material may be released in a nuclear accident or sometimes during normal operation of a nuclear power plant. However, consequence analyses related to radioactive releases are often performed neglecting the particle nature of the release. The properties of the particles have an important role in the radiological hazard. A particle deposited on the skin may cause a large and highly non-uniform skin beta dose. Skin dose limits may be exceeded although the overall activity concentration in air is below the level of countermeasures. For sheltering purposes it is crucial to find out the transport range, i.e. the travel distance of the particles. A method for estimating the transport range of large particles (aerodynamic diameter $d_a > 20$ μm) in simplified meteorological conditions is presented. A user-friendly computer code, known as TROP, is developed for fast range calculations in a nuclear emergency.

CONTENTS

1 INTRODUCTION

Radioactive releases into air from nuclear facilities contain not only gaseous species but also radioactive particles. 'Hot particles' were found after the nuclear weapon tests carried out by the U.S.A., former U.S.S.R., China and France. Radioactive particles (activity up to 300 Bq and diameter less than 15 μm) were found in Japan after the U.S.S.R. nuclear test in September-October 1961 (Mamuro et al 1965a). Particles with a somewhat lower specific activity (activity up to 500 Bq but diameter up to 20 μm) were found in Japan after the first Chinese nuclear test explosion in October 1964 (Mamuro et al. 1965b). Debris from numerous tests of nuclear weapons were found also in Sweden (Sisefsky 1961). The particles were smaller than 5 μm in diameter and their activity was up to 50 Bq (after a cooling time of 120 d).

In addition to nuclear weapon tests, radioactive particulate material has been found after nuclear power plant accidents. In 1957, radioactive particulate matter was found near the Windscale nuclear power plant after a core fire. The total beta activity of individual particles was 37 - 4800 Bq (Sandalls et al. 1993). In the Chernobyl accident in 1986, 6000- 8000 kg of small radioactive particles were dispersed over Europe (Sandalls et al. 1993). They were either monoelemental (or bielemental) particles or multielemental fuel fragments. The particles were even hundreds of micrometers in size and their activity was up to a few MBq's (Salbu et al.1994). Recently, after the incident at Sosnovyy Bor nuclear power plant a few small radioactive particles were found in Finland (130 km from the source) (Toivonen et al. 1992). Particles were smaller than 1 μm and their activity was less than about 1 Bq.

Radioactive particles are also produced and sometimes released during normal operation of nuclear power plants (UNSCEAR 1993). The beta activity of particles may be on the level of tens of MBq's (Mandjoukov et al. 1994). These objects that may be large (a few mm) are classified into metallic activation particles and fuel fragments. Radioactive particles may be released accidentally (due to fires or explosions) also from facilities that handle radioactive material (e.g. reprocessing plants).

The references cited above show direct evidence of radioactive particles found after a release. Some elements (e.g. Ce and Zr) are always in the form of particles. The frequent occurrence of ^{95}Zr and $^{141,144}Ce$ in minor releases from nuclear facilities shows indirectly that at least part of the released material is in particulate form. Thus, monitoring systems for identifying the particles are needed.

Monitoring of released radioactive material is closely connected to the state (gases or particles), elemental properties (volatility), amount (inventory) and behaviour (deposition) of the element considered. In addition, the decay mode of nuclides is of importance. For example, pure beta or alpha emitters can be detected only using tedious sample preparation procedures. Gaseous or volatile species are easily released even during normal operation of nuclear power plants. In a nuclear accident they can be released at the early stages of the accident.

Noble gases and part of iodine may be in the gaseous form whereas other species are in particulate form. Non-volatile elements can be released in fragmentation processes. Due to efficient retention mechanisms in a given release path only small amounts of radioactive particles are usually detected in a release plume. Noble gases are not deposited. However, large particles may be released during a nuclear accident, provided that the consecutive safety barriers are broken.

Environmental monitoring of airborne radioactive substances is conventionally based on air sampling or on-line dose rate measurements. In the case of aerosol sampling, gamma spectrometric methods are used in radionuclide identification. Dose rate measurements of external radiation by Geiger counters do not identify nuclides. Gaseous radioactive species are monitored using special methods. However, these methods do not identify whether the radioactive substances are in the gaseous form or as particles. Other methods (autoradiography, impactors) are needed.

Traditional monitoring techniques in connection with the frequency of nuclear incidents (incidents are more common than accidents; highly radioactive particles are detected mainly after major nuclear accidents), may lead to slightly erroneous interpretation of the significance of radioactive particles. That is, releases from nuclear power plants are considered as 'Becquerels' that are dispersed in the environment, not as radioactive material that is mainly in the particulate form. The significance of this difference is briefly discussed below.

Although the possible existence of highly radioactive particles in a release plume is generally realized, their effect on emergency planning is often less pronounced and sometimes totally omitted. In radiation protection and emergency preparedness large radioactive particles pose different problems than small radioactive particles or gaseous fission products. These problems are clearly seen in operational air concentration measurements. The average nuclide concentration (Bq m^{-3}) is not meaningful if all the activity comes from a few particles. Moreover, the radiological risks related to these highly radioactive particles are not the same as in homogeneous exposure. In a complex three-dimensional wind field, large particles can also be transported to other areas than gases or small particles.

The monitoring networks, which are employed in several countries and designed to detect environmental airborne radioactivity, measure the average activity concentration (Bq m^{-3}) in air or the concentration integral of radionuclides. Single particles are not registered. Afterwards, however, the existence of large radioactive particles can be verified in autoradiography.

A similar situation is met in a typical consequence analysis when statistical models, e.g. Gaussian type models like the 'tilted plume model' (Underwood 1990) are used. The predictions of these models are of statistical nature. The particulate nature of matter is taken into account by using higher values for the deposition velocity (usually 0.01 m s^{-1}). In a case where the average activity concentration actually consists of a few large particles, the interpretation of the calculated results can be misleading. One may ask what does the calculated average concentration (Bq m^{-3}) or fallout (Bq m^{-2}) mean if the activity is in large particles whose number concentration is low. For example, after the incident at Sosnovyy Bor nuclear power plant in 1992 (Toivonen et al. 1992) we found four particles in a filter through which 900 m^3 of air had flown.

Nevertheless, statistical models are useful (with respect to safety analyses of large particles) if activity concentration (Bq m^{-3}) or fallout (Bq m^{-2}) are expressed in terms of number concentration (m^{-3}) or number of deposited particles (m^{-2}). The specific activity of particles considered in the dispersion calculation is then needed. The number concentration or number of deposited particles can be used in estimating the deposition probability onto the skin, for example. The problem is that the results of the statistical models are then adequate only for the particle size determined by the deposition velocity. Dispersion calculations for other particle sizes must be performed separately.

The dose conversion factors (Sv Bq^{-1}) for inhalation are defined for small particles (AMAD = 1 μm). This may be relevant for caesium and iodine but not for non-volatile elements like zirconium and cerium in large particles. The results of the analyses are usually interpreted as being an averaged value for the quantity considered, e.g. the effective dose. The overall activity concentration in air may be below the level of countermeasures. However, there is a risk that a severe local injury may be caused by a single hot particle deposited on the skin or in the upper airways.

Although the released particles are small, they are an intense source of radiation. Skin dose limits may be exceeded due to single particles deposited on the skin. A uranium fuel fragment of size 40 μm can in one day exceed the NCRP limit 10^{10} total beta emissions (NCRP 1989) of acute skin damage, provided that the particle is deposited on the skin (Pöllänen and Toivonen 1994a). ICRP skin dose limit (ICRP 1990) for the public (50 mSv at skin depth of 70 μm averaged over 1 cm^2) is exceeded in one day for a uranium fuel particle of 10 μm in diameter. After the

Chernobyl accident nearly monoelemental ruthenium particles were found (Osuch et al. 1989). Their total beta activity for ruthenium isotopes was up to 200 kBq's. NCRP limit for this particle is exceeded in twelve hours. These particles can be transported hundreds of kilometres from the plant.

In estimating the radiological hazard caused by large particles, the concept of transport range is introduced. It is the horizontal distance between the release point and the point of deposition to the ground. Here, the travel distance of a particle is defined as the length of the curvilinear path in x-y plane. The transport range and the travel distance are equal provided that wind direction is constant during the transport.

For sheltering purposes it is crucial to find out the maximum transport range of particles that can cause an acute health risk, i.e. the areas of particle deposition must be identified beforehand. It is important that travel distances can be evaluated during a nuclear emergency, too. This may lead to identification of fall-out areas.

A method for estimating the transport range of particles is presented in this study. Range estimates are based on the time difference between the release and deposition. During this time the particles, originally lifted up to the effective release height, are transported over a distance determined by the wind velocity. Particles are deposited due to sedimentation and turbulent dispersion.

A user-friendly computer code, known as TROP, has been developed for the estimation of the transport range of large particles. The code is intended mainly for the use in emergency preparedness but it can be used for research purposes, too. TROP is coded using the Visual Basic application development system. The minimum hardware configuration is an IBM compatible microcomputer with a 80386 CPU and internal storage of 4 MB.

The versatile presentation capabilities of the code enable fast and flexible visualization of the results using a graphical WINDOWS interface. Transport range as a function of particle size can be presented in numerical form or as a figure. Graphical output on digitized maps is offered additionally.

2 TRANSPORT RANGE OF PARTICLES

Radioactive material released from a nuclear power plant during a severe nuclear accident can rise up to the height of a few kilometres due to the initial momentum of the plume and the thermal energy available. The fireball of a nuclear detonation may lift surface material and radioactive substances tens of kilometres above the ground. Radioactive particles are then transported thousands of kilometres within air currents. Large particles settle down rather quickly but small particles can stay in the atmosphere for days or even weeks.

Different deposition mechanisms remove particles from the atmosphere. In this study only dry deposition is considered. Dry deposition velocity, v_{dep}, is the effective velocity of particle migration to a surface, i.e.,

$$v_{dep} = J_0 / C_0 , \qquad (1)$$

where J_0 is the particle flux to the ground and C_0 is the undisturbed concentration above the ground. The dry deposition velocity of particles depends on particle properties (size and density), surface characteristics (roughness) and atmospheric conditions. Van der Hoven (1968) suggests that, when the gravitational settling velocity of the particles is greater than 1 m s^{-1} (aerodynamic diameter $d_a > 250$ µm), the particles fall so fast that turbulent dispersion is no longer important. Small particles ($d_a < 1$ µm) are deposited as a result of turbulent dispersion and Brownian motion. When $d_a > 10$ µm the gravitational settling is important (Hanna et al. 1982).

The particles considered here ($d_a > 20$ µm), known henceforth as large particles, have a settling velocity greater than 0.01 m s^{-1} which is the value often used for dry deposition (e.g. in Nordlund et al. 1985). Particles of this size are deposited mainly due to sedimentation or turbulent dispersion. The role of sedimentation and turbulent dispersion in the transport of the large particles is different. Sedimentation moves particles out of the gaseous plume whereas turbulent dispersion spreads both the gaseous plume and the 'particle plume'. Therefore, the behaviour and the radiological consequences of the large particles are not described properly by assuming that the 'particle plume' is mixed in the same way as the gaseous plume (Fig. 1). Deterministic particle trajectory calculations are needed.

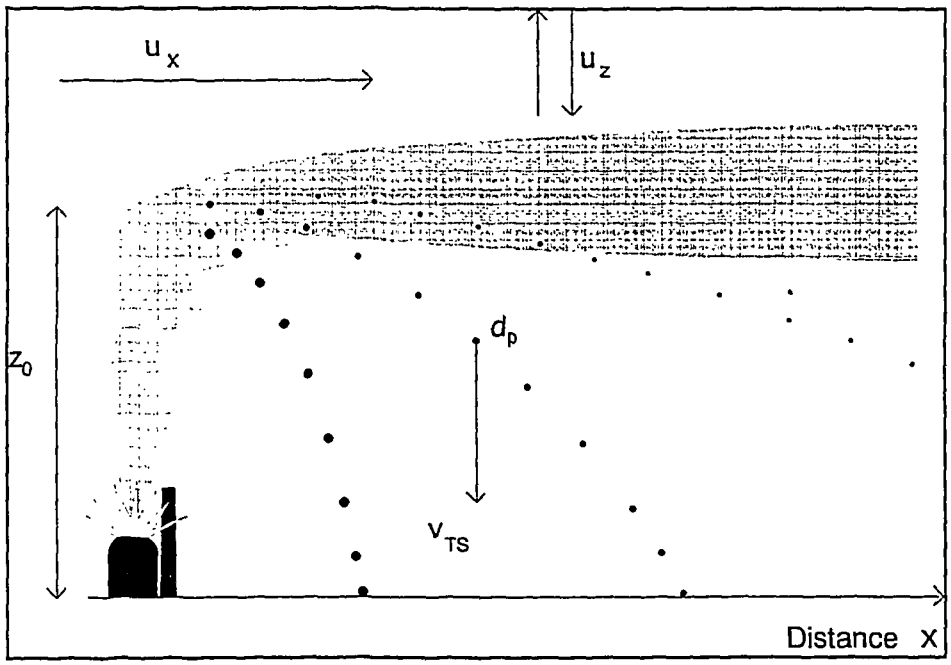

Fig. 1. *Particles of different sizes in a release plume. Particles in a gaseous plume rise to the effective release height, z_0. Large particles leave the main aerosol stream mainly by sedimentation (v_{TS}, is the sedimentation velocity, for the particle of diameter d_p) whereas small particles stay in the plume for a longer time. Horizontal wind velocity, u_x, and vertical wind velocity, u_z (upward or downward), together with sedimentation velocity have an influence on the transport range of the particles.*

In simplified meteorological conditions the transport range of large particles can be calculated as follows. Let us assume that a particle is originally at the height of z_0. Deposition to the ground occurs after the time of

$$t = z_0 / v_{TS} , \qquad (2)$$

where v_{TS} is the sedimentation velocity. Provided that wind direction is constant during the transport, the travel distance, i.e. the transport range, is then

$$x = t\, u_x = z_0\, u_x / v_{TS} , \qquad (3)$$

where u_x is the horizontal wind velocity.

Vertical velocity of air, u_z, may have an essential influence on the range of particles. Provided that u_z is constant during the transport,

$$x = z_0\, u_x / (v_{TS} + u_z) , \qquad (4)$$

where u_z is positive for downward air flows and negative for upward air flows.

Wind conditions may change during the transport. Moreover, sedimentation velocity is a complicated function of particle size. It depends on the density and viscosity of the air, too. A numerical approach is needed.

3 GRAVITATIONAL SETTLING

A brief summary of gravitational settling is described below. A more comprehensive description can be found in the textbooks of aerosol physics (e.g. in Hinds 1982).

The air flow around a freely falling particle is characterized by the Reynolds number

$$Re_p = \frac{\rho_{air}\, v_{TS}\, d_p}{\eta}, \qquad (5)$$

where d_p is the Stokes diameter of the particle and ρ_{air} and η are the density and viscosity of air, respectively. Sedimentation velocity, v_{TS}, depends on the particle size and air properties. In Stokes regime, when $Re_p < 1.0$, the terminal settling velocity is

$$v_{TS} = \frac{\rho_p\, d_p^2\, g}{18\, \eta}, \qquad (6)$$

where g is the acceleration of gravity and ρ_p is the density of the particle.

Let us denote

$$C_D Re_p^2 = \frac{4\, \rho_{air}\, \rho_p\, d_p^3\, g}{3\, \eta^2}. \qquad (7)$$

When $0.05 < Re_p < 4$, the equation (Davies 1945)

$$v_{TS} = \frac{\eta}{\rho_{air}\, d_p} \left(\frac{C_D Re_p^2}{24} - 2.3363 \cdot 10^{-4} (C_D Re_p^2)^2 + 2.0154 \cdot 10^{-6} (C_D Re_p^2)^3 - 6.9105 \cdot 10^{-9} (C_D Re_p^2)^4 \right) \qquad (8)$$

can be applied. When $3 < Re_p < 10000$, the equation

$$v_{TS} = \frac{\eta}{\rho_{air}\, d_p} \cdot 10^A , \tag{9}$$

where

$$\begin{aligned} A = &- 1.29536 + 0.986 \log_{10}(C_D Re_p^2) \\ &- 0.046677 \log_{10}(C_D Re_p^2)^2 \\ &- 0.0011235 \log_{10}(C_D Re_p^2)^3. \end{aligned} \tag{10}$$

can be used for the settling velocity (Davies 1945).

It is often convenient to use the particle aerodynamic diameter, d_a, instead of the Stokes diameter, d_p, i.e. the analysis is made for a unit density sphere having the same settling velocity as the particle considered (Fig. 2). Generally, the relationship between d_p and d_a is defined by equating the settling velocities of the particles. The two diameters are coupled in the Stokes regime by

$$d_a = d_p \, (\rho_p/\rho_a)^{1/2} . \tag{11}$$

Outside the Stokes regime, equation 11 is not valid. Serious errors are made in the transport range calculation (Barla and Bayülken 1991) if the sedimentation velocity in equation 6 is used beyond its application regime.

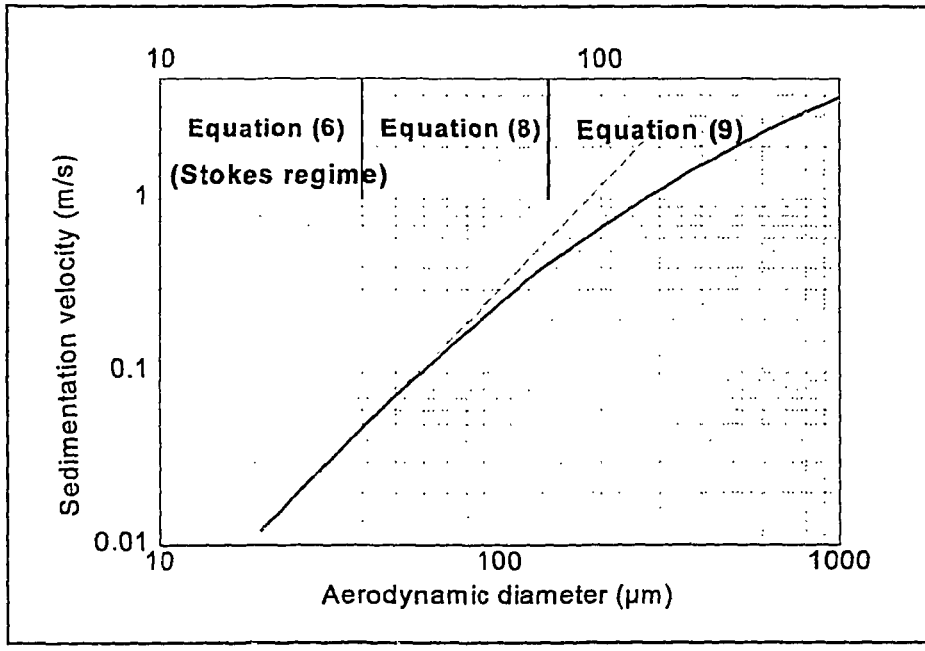

Fig. 2. *Sedimentation velocity as a function of particle aerodynamic diameter. Outside the Stokes regime, equation 6 is not valid (dashed line). Approximative validity regimes of equations 8 and 9 are shown, too.*

4 TURBULENT DISPERSION

Turbulent dispersion is described e.g. in references (Hanna et al. 1982) and (Slade 1968). Some qualitative points regarding large particle transport are discussed here.

The dispersion of airborne material is a function of the intensities of turbulent fluctuations in the atmosphere. The temporal evolution of the mixing layer height depends on the equilibrium of the vertical turbulent fluxes. In dispersion modelling, the fluxes have to be parametrized because no measurements are routinely available. In addition, the turbulent diffusion is basically a highly non-linear phenomenon and thus, in contrast to the gravitational settling, only statistical properties of the turbulent flows can be predicted. The steady-state equilibrium between the kinetic and thermal parts of turbulence is usually called atmospheric stability.

The transport range of large particles depends on the vertical component of turbulence. During the settling, the particles are transported within air that is moving periodically upwards and downwards due to vertical turbulence. These vertical velocities determine the net settling velocity, i.e. the sedimentation velocity with respect to the ground surface (the settling velocities given by equations 6, 8, and 9 are for still air).

A particle that moves in varying wind conditions does not perfectly follow the small scale eddy motion of air. The relaxation time, τ_p, characterizes the time required for a particle to adjust its velocity to new conditions of forces (Table I). In the Stokes regime, when $Re_p < 1$,

$$\tau_p = \frac{\rho_p \, d_p^2}{18 \, \eta} \, . \qquad (12)$$

Instantaneous vertical velocitites of turbulent air (microscale turbulence) can be high, far higher than typical bulk vertical velocities. Small particles follow the streamlines fairly well whereas large particles are deviated more (Fig. 3). A particle is not sensitive to turbulent vertical flows, provided that the characteristic time of fluctuating flows is considerably shorter than the relaxation time of the particle.

Table I. *Relaxation time and terminal settling velocity as a function of particle aerodynamic diameter (Davies 1977).*

Diameter (μm)	Relaxation time (s)	Settling velocity (m s^{-1})
1	$3.57*10^{-6}$	0.000035
10	$3.06*10^{-4}$	0.003
20	$1.22*10^{-3}$	0.012
50	$7.34*10^{-3}$	0.072
100	$2.55*10^{-2}$	0.25
200	$7.14*10^{-2}$	0.70
500	$2.04*10^{-1}$	2.0
1000	$3.93*10^{-1}$	3.85

Up to the distances of tens of kilometres the release plume is dispersed mainly due to microscale and mesoscale turbulence. Although the instantaneous vertical velocities in turbulent air can be high, the net spread of the plume is substantially smaller than would be expected from these instantaneous velocities. In this study, the particles are assumed to be dispersed by turbulence in the same way as particles that have no inertia. In reality the plume of monodisperse large particles is spread less than the plume consisting only of small particles and gases, i.e. the behaviour is more deterministic than assumed here.

As pointed out above, deterministic range analyses are needed in estimating the significance of large particles with respect to acute health effects, sheltering purposes, and fast identification of fall-out areas. How to take into account the statistical nature of turbulent flows in deterministic analyses? In the present analysis the concept of effective vertical velocity of air, u_z, is introduced.

For large-scale vertical movements of air (synoptic scale weather systems) the effective large-scale vertical velocity of air, $u_{z,l}$, can be calculated from the wind fields. It is simply the upward or downward velocity of air during the particle transport. However, in case of microscale and mesoscale turbulence the effective vertical velocity is chosen in a different way. The Pasquill classification scheme

(Pasquill 1961) (or other classifications), together with Briggs formulas (Briggs 1973) (or others) for plume width, give us a possibility to use a 'semi-deterministic' procedure to estimate the effects of turbulence on the transport range of large particles. In this paper the choice is made using a spreading velocity of the (gaseous) plume, i.e. the effective vertical dispersion velocity of the plume, $u_{z,t}$.

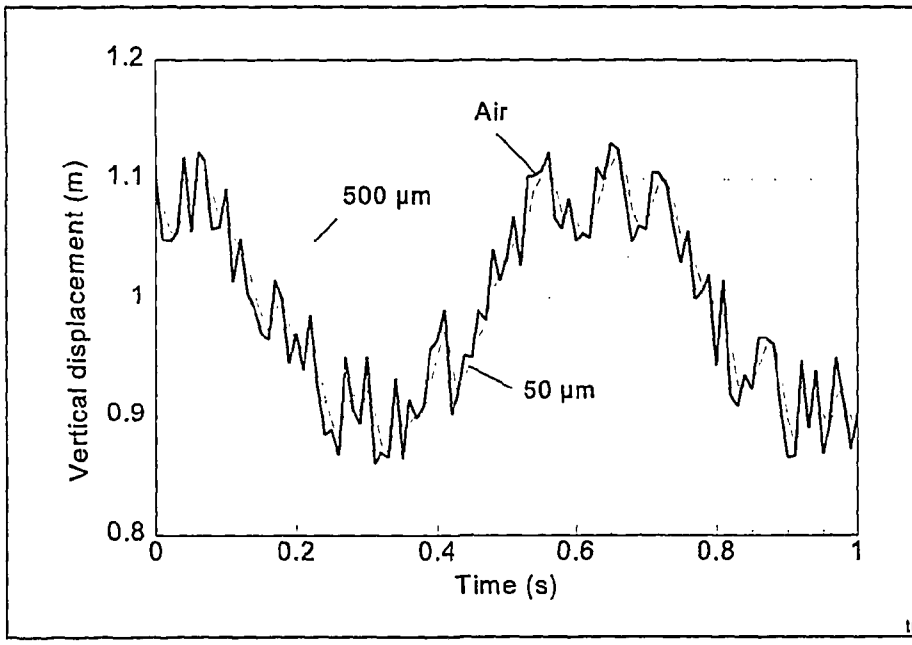

Figure 3. *Schematic behaviour of particles in microscale turbulent air (neglecting sedimentation). Vertical turbulence (1 m above ground) is created using a random number generator. Characteristic time of the turbulences (solid sawtooth line) are 0.01 s and 0.5 s (sinusoidally varying background). Vertically fluctuating displacements are typical for turbulent air (see e.g. Joffre 1983). Particles with aerodynamic diameter of 50 µm (dashed line,* τ *= 0.00734 s) and 500 µm (dotted line,* τ *= 0.204 s) tend to follow vertical air flows whose characteristic time is larger than* τ.

In practice, there is no need to distinguish between the components of the effective vertical velocity. The effective vertical velocity, u_z, is the sum of the large scale and small scale vertical velocities

$$u_z = u_{z,l} + u_{z,t} . \qquad (13)$$

The influence on the particle transport by the small scale vertical movements of the air is analyzed using parametric equations derived for certain classified weather conditions (Pasquill classes). Parametric expressions are easy to use in calculations. Here the effective vertical velocity, $u_z = u_{z,t}$, is assumed to be of the same order of magnitude as the change in the vertical 'depth' of the plume as a function of time. The dispersion parameter, σ_z, is the standard deviation of the Gaussian distribution in the vertical direction. In the present analysis the vertical spreading rate of the plume is assumed to be proportional to the change of σ_z per unit time. In this case the effective vertical dispersion velocity, $u_{z,t}$, is estimated from the time derivative of the vertical dispersion parameter, $\sigma_z(x)$

$$u_{z,t}(x) = \frac{d\sigma_z(u_x t)}{dt} \qquad (14)$$

The interpretation of $u_{z,t}$ is obvious: it is the spreading velocity of the plume (the width of one standard deviation) due to atmospheric turbulence in the Pasquill class considered.

5 TROP CODE

TROP is a code that can calculate the Transport Range Of large Particles of different sizes in simplified atmospheric conditions. Particles are assumed to deposit mainly due to gravitational settling. The effects of turbulent dispersion on the ranges are taken into account using the concept of effective vertical velocity of air. Range calculations are based on the time difference between the release and the deposition on the ground. During this time the particles are transported over a distance determined by the wind velocity.

TROP is intended for use in emergency preparedness and in research. Thus, the presentation capabilities are as versatile as possible. Transport ranges as a function of particle size can be presented either in numerical or in graphical form. Ranges can be presented also on a digitized map. The results calculated by the code supplemented, if necessary, by three-dimensional particle trajectories calculated by the TRADOS code (Valkama and Salonoja 1993), allow real-time identification of areas where large particles may be deposited.

TROP has only one input window (Fig. 4). The main input parameters are:
- models for the atmosphere,
- wind conditions, i.e. horizontal and vertical wind velocities,
- particle characteristics (particle sizes and density),
- time step,
- test particle printout, and
- effective release height.

In estimating the effects of varying air properties three models for the atmosphere can be used in transport range calculations. The Simple model is intended to be used for low altitudes and steady atmospheric conditions. Wind velocities and air properties remain constant during particle settling. The model using properties of standard atmosphere is suitable for high release heights. Properties of air vary as a function of altitude but horizontal and vertical wind speed are constant during the particle settling. The 'real' atmosphere refers to more realistic weather conditions. Like in the simple model, NTP conditions are assumed for air, but horizontal wind speed near the ground varies as a function of altitude.

The code checks the overall validity of the input values. Horizontal wind velocity must be below 20 m s^{-1}. In the 'real' model the Pasquill classes depend on the wind speed. The density of a particle should be 1000 - 20000 kg/m^3. Particle Stokes diameter should be 5 - 1000 μm (lower limit is determined in such a way that sedimentation velocity of 1 cm s^{-1} is exceeded). Ranges are calculated for particle

sizes determined by minimum and maximum diameters and the size of the diameter increment (Fig. 4). The effective release height is 50 - 20000 m for the simple and standard atmospheric models and 50 - 3000 m for 'real' weather conditions.

TROP is designed in such a way that the significance of different phenomena can be evaluated in a straightforward manner. The main uncertainties related to transport range calculations are due to insufficiently known properties of particles and atmosphere. Sedimentation velocity depends strongly on particle size but this dependency is well known. TROP calculates transport ranges simultaneously for a set of user-defined particle sizes, not for one size only. However, the uncertainties connected to varying atmospheric conditions are estimated using a different approach.

Vertical movements of air have a strong influence on the transport ranges of particles (at least for the smallest particle sizes considered in TROP). In practice, the estimation of the vertical flows is difficult without accurate meteorological data. To estimate the uncertainties related to varying wind conditions, the ranges are calculated simultaneously for three identical particles. No vertical air flows are assumed for one of these particles. The other particles move either in upward (larger transport range) or in downward (smaller transport range) vertical air flows.

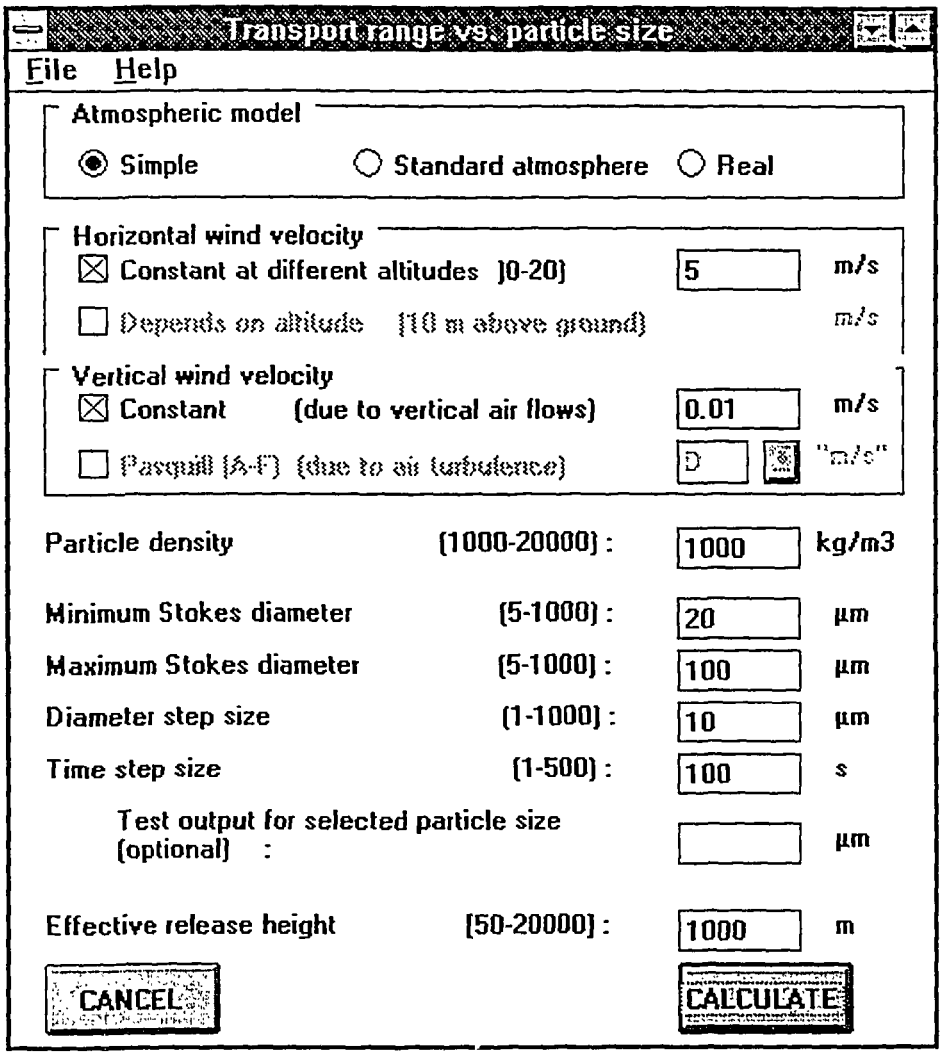

Figure 4. *Input window of the TROP code. Default values shown on the screen are: simple atmospheric model, horizontal wind velocity 5 m s^{-1}, vertical wind velocity (directed upwards and downwards) 0.01 m s^{-1}, density of a particle 1000 g cm^{-3}, and effective release height 1000 m. Ranges are calculated for particles with diameter of 20 ,30, ...,100 µm.*

5.1 Models for the atmosphere

The effects of vertical air flows are modelled using the concept of effective vertical velocity of air. As mentioned previously, ranges are calculated simultaneously for three identical particles (for each particle size in a set). One particle moves in zero vertical wind flows. For this particle sedimentation is the only deposition mechanism. Vertical air flows are not neglected for the other two particles. They move in upward directed or downward directed effective vertical air flows.

Three different atmospheric models can be used to study the effects of varying air conditions. Effective vertical velocity of air is constant during the particle transport (for particles that move in upward or downward directed air flows) in the simple and standard atmosphere models. For the model using more realistic atmospheric conditions the selection of vertical velocity is based on the spreading velocity of the plume. Some altitude-dependent phenomena are also modelled in a different way.

5.1.1 Simple model

In the simple model, NTP conditions for the atmosphere are assumed. All atmospheric conditions are stationary during the particle transport. Horizontal and vertical air velocities are constant. They depend neither on the altitude nor the distance from the source. Air density and air viscosity are constant, too.

Transport range has an analytical expression in the Stokes regime (equations 3 and 6)

$$x = \frac{18\ \eta\ z_0\ u_x}{\rho_p\ d_p^2\ g}, \qquad (15)$$

assuming no vertical velocity of air. In a real transport situation vertical air flows always exist. During the travel time, the particles move up or down faster or slower, depending on the direction of the effective vertical velocity, $u_z = u_{zj}$. The net settling velocity is changed to $v_{TS} + u_z$, where u_z is negative for upward air flows and positive for downward air flows. Transport range is now (equations 4 and 6)

$$x = \frac{18\ \eta\ z_0\ u_x}{\rho_p\ d_p^2\ g \pm 18\ \eta\ z_0\ u_z}. \qquad (16)$$

Beyond the Stokes regime the calculations have to be performed numerically. Numerical calculations are needed, too, when standard atmosphere and real models are used.

5.1.2 Standard atmosphere

In the model of standard atmosphere the properties of air vary as a function of the altitude, z. This is the only difference with respect to the simple model. In practice, the simple and standard models give nearly equal results at low altitudes. Sedimentation velocity is larger at high altitudes than near the ground. Ranges are then somewhat shorter than in the simple model, provided that wind speed is equal during the particle transport. Air density and air viscosity have an influence on the sedimentation velocity (equations 6, 8, and 9).

The average adiabatic decrease of air temperature is (Hanna et al. 1982)

$$\Delta T/\Delta z = -6.5 \ K/km. \qquad (17)$$

Air temperature at the ground level is 288 K. Dynamic viscosity of air, η (kg $s^{-1}m^{-1}$), depends on the absolute temperature (Rogers and Yau 1989)

$$\eta = 1.72 * 10^{-5} \ (\ 393 \ / \ (T + 120) \ ) \ (\ T \ / \ 273 \ )^{3/2} \ . \qquad (18)$$

Air pressure, P (Pa), decreases as (Kyle 1991)

$$P = P_0 \ e^{-(z/H)} , \qquad (19)$$

where $P_0 = 1013$ hPa (atmospheric pressure at the ground level) and $H = 7.995$ km is the scale height for isothermal atmosphere. Density of air, ρ_{air} (kg m^{-3}), comes from the equation of state for dry air

$$\rho_{air} = P \ / \ R' \ T \ , \qquad (20)$$

where $R' = 287$ J kg^{-1} K^{-1}.

Horizontal and vertical air velocities are constant during the transport. Because in reality the horizontal wind speed is a function of the altitude, the user must select such a speed that is prevailing during the settling (e.g., average wind speed), not necessarily the wind speed prevailing at the ground level.

5.1.3 Realistic weather conditions

The more realistic model can be used only for release heights lower than 3000 m. The density and viscosity of air are constant (this is a good approximation in low altitudes). However, vertical variation of the horizontal wind velocity is given by the power law (Hanna et al. 1982)

$$u_x(z) = u_{10m} \, (\, z \, / \, 10 \,)^{I} \, , \qquad (21)$$

where u_{10m} is the wind speed measured ten meters above the ground and z (m) is the height. Exponent I (Irwin 1979) depends on the stability class (Table II). Equation 21 is valid up to about 200 m above the ground. For higher altitudes the horizontal wind velocity is assumed to be constant, i.e. it has the same value as at the height $z = 200$ m. User can specify the stability class within the limits of wind velocity.

Table II. *Limits of wind speed at the level of 10 m, the value of exponent I, vertical dispersion parameter σ_z (Hanna et al. 1982) and vertical spreading velocity of the plume, u_z, in different Pasquill classes.*

Stab. class	Wind speed (m s^{-1})	I	σ_z (m)	u_z (m s^{-1})
A	0 - 2	0.07	$0.20\,x$	$u_x\,0.20$
B	0 - 5	0.07	$0.12\,x$	$u_x\,0.12$
C	0 - 6	0.10	$0.08\,x\,(1+0.0002\,x)^{-1/2}$	$u_x(\sigma_z - 0.16\sigma_z^3/x) / x$
D	0 - 20	0.15	$0.06\,x\,(1+0.0015\,x)^{-1/2}$	$u_x(\sigma_z - 0.208\sigma_z^3/x) / x$
E	0 - 5	0.35	$0.03\,x\,(1+0.0003\,x)^{-1}$	$u_x(\sigma_z - 0.010\sigma_z^2/x) / x$
F	0 - 3	0.55	$0.016\,x\,(1+0.0003\,x)^{-1}$	$u_x(\sigma_z - 0.019\sigma_z^2/x) / x$

Upward and downward air velocities are assumed to be equal to the vertical spreading velocity of a gaseous plume (the spread of one standard deviation, directed both upward and downward). Effective vertical velocities are calculated using equation 14. These velocities are dependent on horizontal distance, horizontal wind velocity, and Pasquill class (Table II). Note that the vertical dispersion parameters in Table II represent open-country conditions at short distances (0.1 - 10 km). However, an extrapolation up to 100 km is sometimes used. Additionally, a constant vertical velocity can be selected. The total vertical velocity is the sum of the spreading velocity and the constant vertical velocity (equation 13).

The vertical dispersion parameter, σ_z, is only a function of distance, x (Fig. 5). However, the vertical spreading velocity, u_z, is a function of horizontal wind velocity, u_x. To cancel out the effects of wind velocity the spreading velocity in Fig. 6 has been divided by the wind speed.

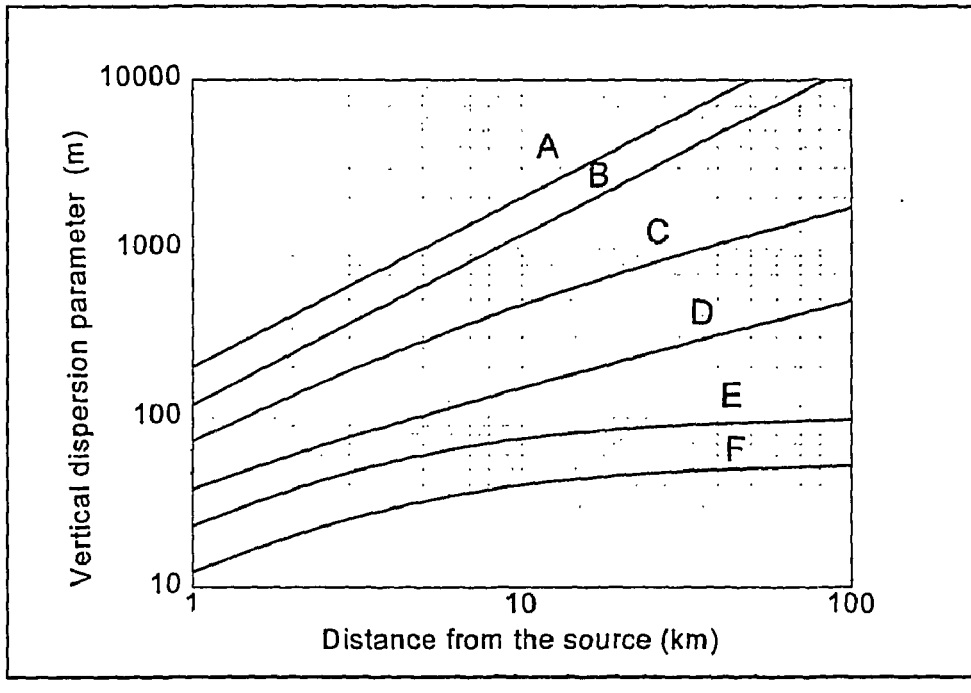

Figure 5. *Vertical dispersion parameter, σ_z, in Pasquill classes A - F as a function of distance from the source.*

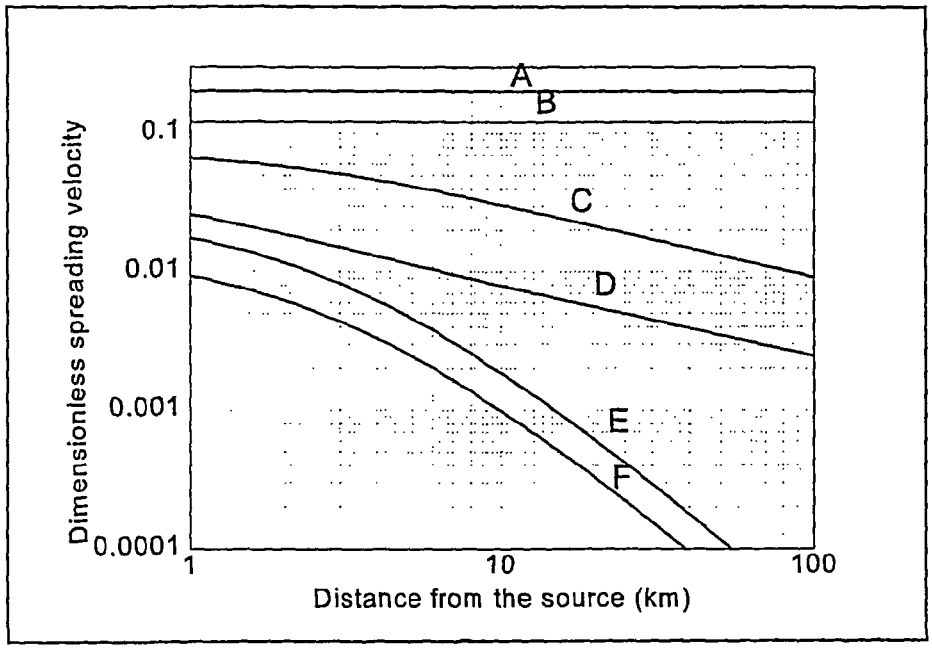

Figure 6. *Dimensionless spreading velocity, u_z/u_x (the spread of one standard deviation, see text), of the plume in Pasquill classes A - F as a function of distance from the source. Wind speed is 1 m s^{-1}. Spreading velocity for other horizontal wind velocities is obtained by multiplying the value in y-axis by u_x.*

5.2 Numerical scheme

The initial coordinates (in x-z coordinate system) of the particle are (x_i,z_i). The true sedimentation velocity of the particle is $v_{TS} + u_z$, where u_z is either positive (downward velocity), negative (upward velocity) or zero (Fig. 1). At the time t the particle is at the point (x_{i+1},z_{i+1}), where

$$\begin{aligned} x_{i+1} &= x_i + (u_x(z))_i , & i &= 0,1,2,... \\ z_{i+1} &= z_i - [(v_{TS} + (u_z)_i]\Delta t, & i &= 0,1,2,... \end{aligned} \qquad (22)$$

It is assumed that the wind conditions do not change remarkably during a short time interval Δt. After every time step a new location (x_{i+1},z_{i+1}) is calculated until $z_{i+1} \leq 0$.

The accuracy of the results depends on the selected time step. At least for the smallest particle sizes, the calculations may take some time if the time step is too short, whereas a too large time step may lead to inaccurate results. The limits of time step are at present 1 - 500 s. For example, if wind speed is 20 m s^{-1} the particles travel 10 km during a time step of 500 s. If deposition occurs at the very beginning of this time step, an error of about 10 km is generated.

The calculations for particles subject to different vertical wind conditions (see below) are performed simultaneously during each time step.

5.3 Presentation of results

Transport ranges as a function of particle size can be presented numerically (Fig. 8), graphically (Fig. 10), or superimposed on a digitized map (Fig. 11). The default form is a numeric presentation. Graphical presentation and maps can be selected in the window of the numeric presentation (Fig. 8). A test particle printout (Fig. 9) may be used for the verification of the results.

Transport ranges are calculated as a function of particle size. During each execution of the TROP code, three values of transport ranges are calculated (Fig. 8):

RANGE-	transport range for downward vertical velocity of air.
RANGE	transport range for zero vertical velocity.
RANGE+	transport range for upward vertical velocity of air.

TIME-, TIME, and TIME+ are the time differences between the release and the deposition in the downward, zero, and upward directed air flows, respectively.

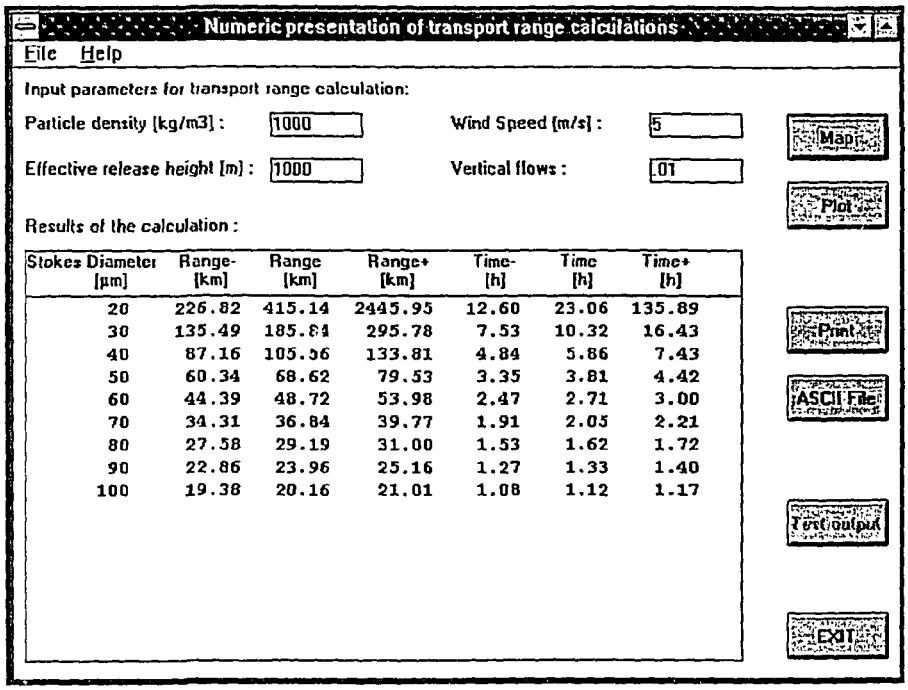

Figure 8. *Numerical presentation of the results.* Map *button displays digitized maps and* Plot *button shows graphical output (Fig. 10). Ranges can be printed to an* ASCII File *or to a* Printer. *An ASCII file is created in the directory specified by the user.* Test output *button shows test particle printout, see Figs. 4 and 9.*

The test particle printout (Fig. 9) enables to get a view of the particle behaviour during the settling process. Location of a particle and atmospheric conditions during the particle settling are followed step by step (the time step determined by the user in the input window). The altitude in Fig. 9 refers to a particle that travels in conditions of "no vertical winds". The test particle printout can be calculated for only one particle size at a time.

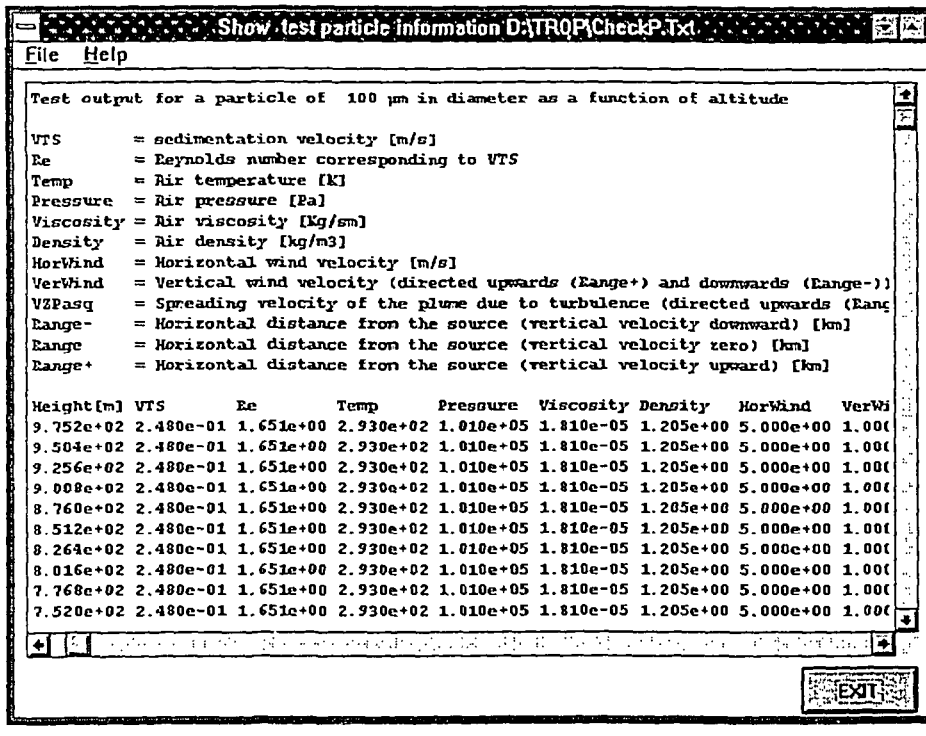

Figure 9. *Test output for a particle of 100 µm in diameter as a function of altitude. Input values are those used in Fig. 4 (atmospheric conditions do not change during the settling).*

Plot command (Fig. 8) creates a figure that displays the transport range as a function of particle diameter (Fig. 10). The curves are for particles in the downward (RANGE-), zero (RANGE) and upward (RANGE+) vertical wind flows. If a zero value is given for the vertical wind velocity, the three curves are then equal.

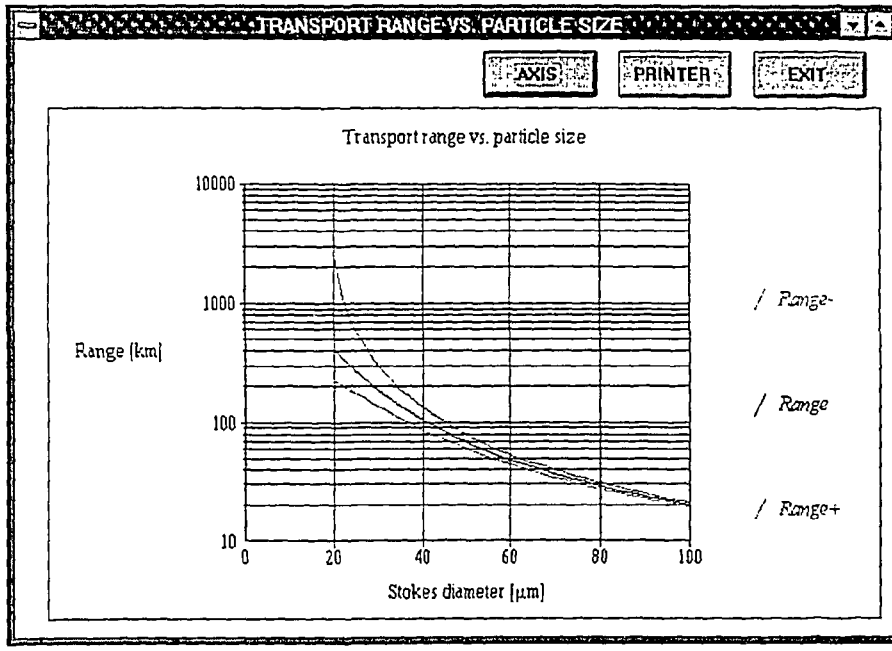

Figure 10. *Transport range (km) as a function of particle diameter for particles in the downward (RANGE-, lower curve), zero (RANGE, curve in the middle) and upward (RANGE+, upper curve) vertical wind flows. The scale of the y-axis, as well as the curve style, can be changed through the* AXIS *button. The figure can be printed by pressing the* PRINTER *button.*

Wind direction is not taken into account in the TROP code. Thus, the ranges are presented as concentric circles on raster maps (Fig.10). The maps are from the Loviisa and Olkiluoto areas. Maps showing Southern Finland, the whole of Finland and northern Europe are included, too. Other maps must be customized.

Operations that can be performed in the map window (Fig 11) are: **Draw** is used for selecting particle ranges and/or particle and air trajectories (see later). The **Insert** option gives a possibility to write text on the map or to draw "hand made" trajectories (using the mouse). An arrow showing a user-defined wind direction may be displayed, too. This feature may be useful in a possible emergency situation. The **Clear** option clears the map. Longitude and latitude, as well as the distance of the cursor from the selected point (e.g. from the Loviisa nuclear power plant), can be shown using the **Options** command.

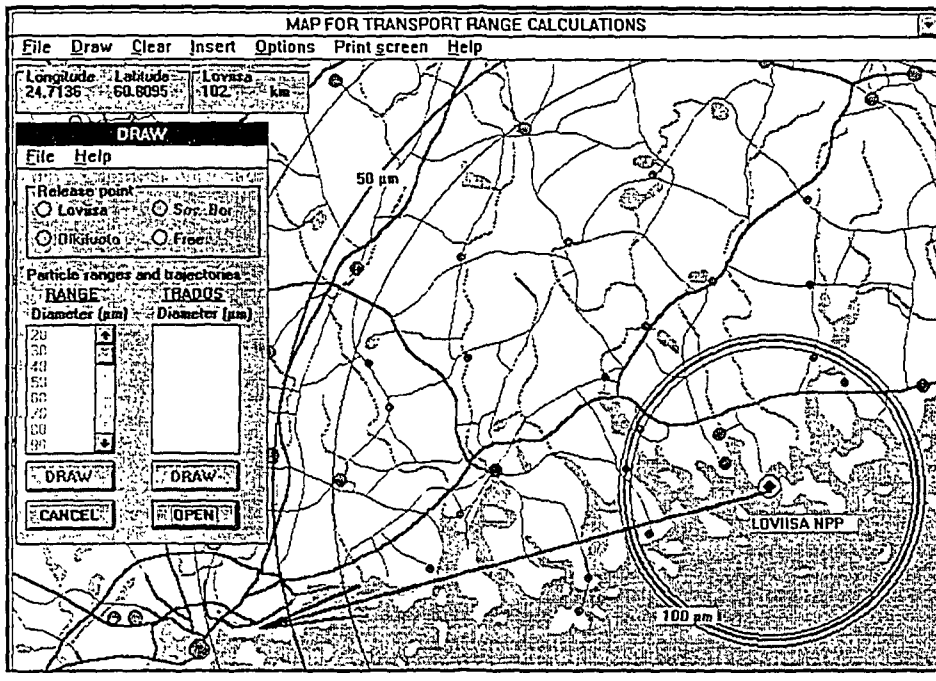

Figure 11. *Transport ranges for 50 µm and 100 µm particles hypothetically released from the Loviisa nuclear power plant (the map of Loviisa area). Input parameters are those presented in Fig. 4. Thick circles represent a particle that moves in zero vertical flows. Thin circles are for the particles experiencing upward and downward directed vertical flows (see the ranges in Fig. 8). Particles are selected using* **Draw** *option. Then a window presented at the left appears. The release point must be selected before the selection of particle sizes. The arrow of wind direction comes from* **Insert** *option. Longitude and latitude as well as distance of the cursor from Loviisa NPP are also from* **Insert** *option.*

6 PARTICLES IN THREE-DIMENSIONAL WIND FIELDS

Large particles are not distributed within the plume in the same way as gaseous fission products or small particles (Fig. 1). Soon after the release the large particles leave the main aerosol stream mainly by sedimentation. In weather types where the wind conditions (wind speed and wind direction) differ significantly at different heights, the large particles and gaseous species or small particles are transported separately (Fig. 12). It is even possible that in some areas the fall-out contains mainly large particles, not gaseous fission products or small particles.

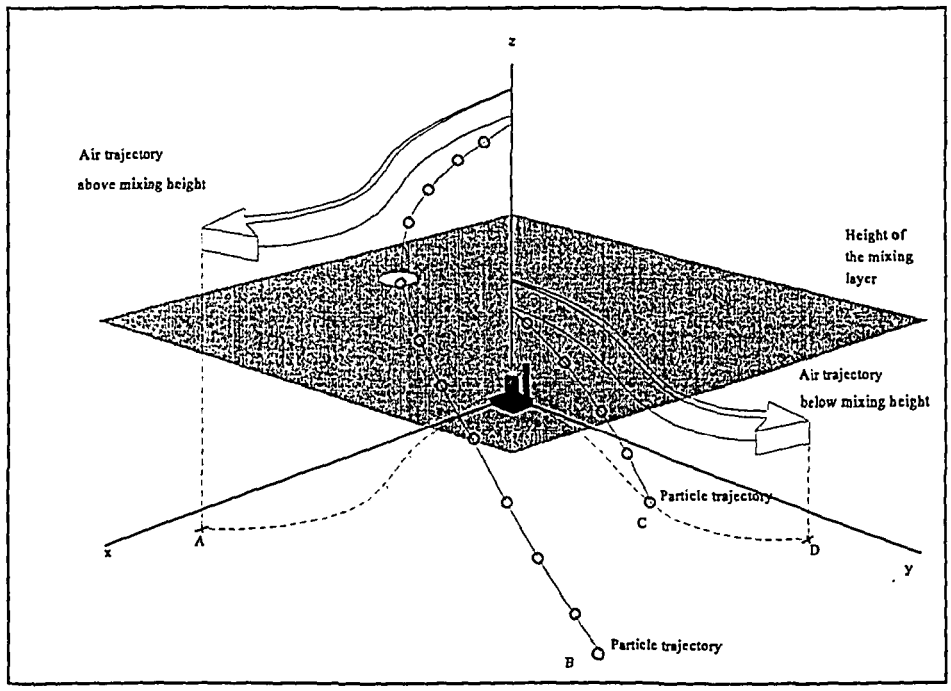

Figure 11. *Hypothetical route of particles and air below and above some mixing height (in x,y,z coordinate system). Wind conditions (speed and direction) differ in both air layers and, consequently, air parcels do not move along the same path. Particles originally above the mixing height behave initially according to the conditions of the upper layer. When they reach the mixing layer they move subject to the conditions prevailing there. Fall-out of particles may vary in different regions. Region (A) contains little or no fall-out whereas region (B) may receive fall-out that contains mainly large particles. Region (C) contains large and small particles, and region (D) small particles.*

The variation of horizontal wind direction and speed with height originates from the fact that the resultant of the forces acting upon an air parcel is different at different heights. In the first 1000 ... 1500 metres above the earth's surface wind speed and direction are determined primarily by three forces: the pressure force (due to the horizontal pressure gradient), the Coriolis force (due to the earth's rotation) and the frictional force (due to the nearness of the earth's surface). The pressure gradient alone would cause the air flow from areas of high pressure to areas of low pressure. Since the earth itself is turning beneath this flow, the Coriolis force tends to turn the observed air flow to the right in the Northern Hemisphere. The net result of the two forces in equilibrium is a flow that is parallell to the isobars with low pressure to the left of the direction of motion. The wind resulting from this balance is called geostrophic wind.

In the upper layers of the atmosphere, observed winds are often quite close to the geostrophic wind. Near the ground, however, a force due to the frictional drag exerted on the atmosphere by the surface disturbs the balance described above. This force not only reduces the wind speed near the surface but also forces the air near the ground to move at some angle (to the left about 15 ... 50 degrees, depending on the type of surface and the time of day) to the geostrophic wind. Above the surface the wind usually turns slowly in a clockwise manner. The angle between the observed wind and the geostrophic wind gradually decreases with height until the observed wind becomes parallell and equal in magnitude to the geostrophic wind. Above this height, i.e. above the atmospheric boundary layer, the wind characteristics are separated from surface influences and mainly reflect the effects of the synoptic weather conditions.

In general, TROP does not fully take into account varying wind conditions during particle transport. Thus, at least for some atmospheric conditions, the transport of large particles must be connected to the prevailing weather conditions. A long-range atmospheric transport, dispersion and dose model TRADOS has been developed by the Finnish Meteorological Institute (FMI) and the Technical Research Centre of Finland (VTT). TRADOS is capable of performing fast real-time calculations in case of a nuclear accident (Valkama and Salonoja 1993).

A trajectory is a path along which an air parcel or a particle moves in the atmosphere. The transport of radioactive material is described in the TRADOS model by 3-dimensional trajectories. The vertical concentration profile is described by the gradient-transfer approach using steady-state K_z-profiles. For each trajectory segment horizontal dispersion, dynamical mixing height and time-integrated air concentration at ground level, as well as dry and wet deposition, can be computed for selected groups of radionuclides. TRADOS uses numerical weather fields received either from FMI's own HIRLAM-model or from the European Center of Medium Range Weather Forecasts (ECMWF) global model.

TRADOS can be used to estimate the transport of hot particles. The particles are assumed to move like an air parcel, except that they sedimentate during the travel. The resultant vertical velocity is the sum of the sedimentation velocity and the velocity caused by the ascending or descending air flow. Unlike air parcel trajectories, the particle trajectory is terminated when it hits the ground. Results of the TROP code (concentric circles) and the TRADOS code (particle trajectories) can be viewed simultaneously in the map window. An appropriate TRADOS output file must be opened using the **Draw** and OPEN operations (release point is not needed, see Fig. 11).

Compared to the air trajectory, the particle trajectory descends to a lower altitude where wind conditions may differ. There the particles move in a different way compared to the air parcel above it. Particle trajectories often closely resemble air trajectories, but sometimes they differ greatly. This is most evident in the presence of strong cyclonic curvature and steep pressure gradients usually associated with weather fronts.

A set of particle trajectories and an air parcel trajectory were calculated by TRADOS using real wind fields (Pöllänen et al. 1993). Transport ranges for the same particle sizes are calculated by TROP using input values presented in Fig. 4 (except that the effective release height $z = 2700$ m and no vertical wind velocity is assumed). The results calculated by TROP and TRADOS are presented in Fig. 13.

Wind direction and horizontal wind velocity varied in different air layers (i.e., wind velocity was not 5 m s^{-1} during the particle transport). These effects are not fully considered in TROP. Fig. 13 shows that the transport range for a $d_a = 40$ µm particle calculated by TROP is equal to the range (trajectory length) calculated by TRADOS. The average wind velocity during particle transport was 5 m s^{-1} (Pöllänen et al. 1993). For smaller particles the average wind speed was lower (down to 3.5 m s^{-1}). and for larger particles higher (up to 6 m s^{-1}). Considering the ranges, both methods give equal results provided that the average wind speed during the particle transport is the same. However, TROP cannot account for the effects of changing wind direction.

Intervention operations (e.g. evacuation) based only on air parcel trajectories may not be adequate in estimating the radiologically hazardous areas. In operational use particle trajectory calculations, similar to air parcel calculations, are needed.

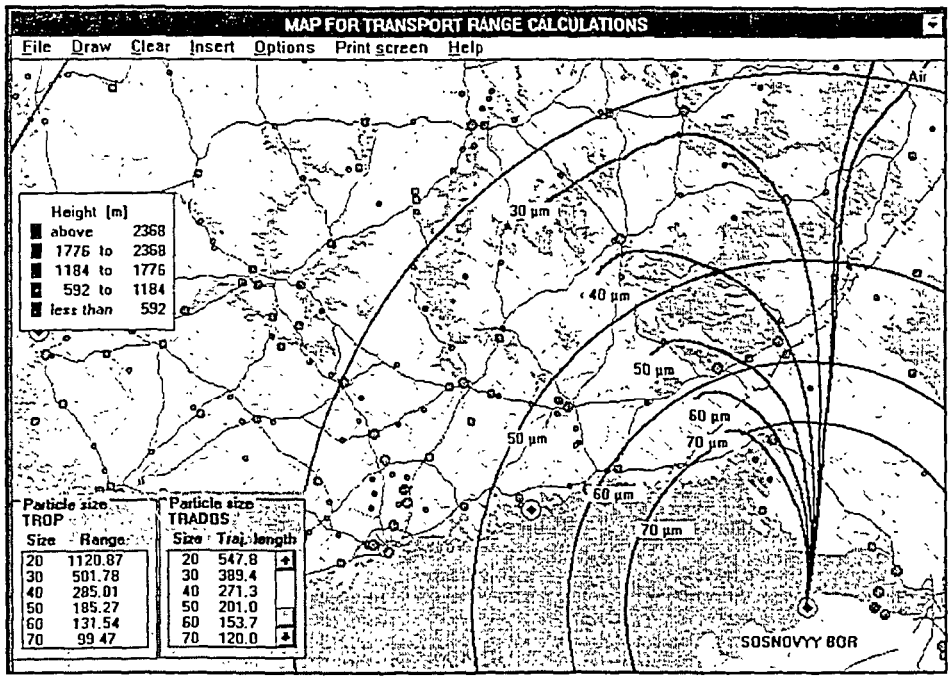

Figure 13. *Trajectories of an air parcel and a group of particles with different aerodynamic diameters calculated by TRADOS. The concentric circles represent TROP calculations for the same particle sizes (in this case vertical velocity, u_p is zero and, thus, only one circle for each particle size is given). Hypothetical particles are released from the Sosnovyy Bor nuclear power plant (the map is of South Finland). Release height is 2700 m. The height of the particles during the transport is marked using different colors. The average wind velocity along the particle trajectories is between 3.5 and 6 m s^{-1}. The transport situation refers to the days 22-24 February 1993. Transport ranges (TROP) and respective trajectory lengths (TRADOS) for the selected particles are shown at the bottom left of the screen. The deviations, especially those for the smallest and largest particle sizes, result from the fact that wind speed differs significantly during the transport. TROP disregards any changes in wind direction.*

7 DISCUSSION

As regards emergency preparedness purposes, it is important to realize the existence of the radiological hazard caused by highly radioactive particles (hot particles). The possibility of a release of these particles in a nuclear accident and, consequently, their transport for hundreds of kilometers from the plant must be considered in the contincency plans.

The methods presented in this study can be used in two ways: (1) If the effective release height of the plume is known, it is possible to estimate the maximum size of the particles that can travel to the specified target area. This information is highly important in identifying the areas that may receive a fall-out containing hot particles. (2) If nuclear fuel particles of certain size are found in the target area, it is possible to obtain an estimate for the true effective release height of the plume. This knowledge is useful in the dispersion studies of the plume in general.

Air parcel trajectories are useful in estimating the transport of gaseous pollutants. During the nuclear incident in Sosnovyy Bor in 1992, trajectory analysis was used successfully to predict the route of the plume (Toivonen et al. 1992). Only three-dimensional trajectory analyses can take into account the actual meteorological conditions and identify the areas where large particles might be deposited.

Before particle trajectory calculations can be performed, the size of the particles and their density must be known. Moreover, the effective release height of the particles must be estimated. Weather conditions during the particle transport may vary, too. In operational use the above mentioned quantities are, of course, very uncertain and the transport ranges calculated by TROP are only suggestive. However, three-dimensional particle trajectories calculated by TRADOS give a good possibility to obtain operational identification of the fall-out areas.

REFERENCES

Barla M C and Bayülken A R. On the importance of the atmospheric parameters in the fission products distribution of a severe reactor accident. Nucl. Saf. 1991; 32: 544-550.

Briggs G A. Diffusion estimation for small emissions. ATDL Contribution File No. 79 (Draft), Air Resources Atmospheric Turbulence and Diffusion Laboratory, NOAA, Oak Ridge, Tennessee, 1973.

Davies C N. Definitive equations for the fluid resistance of spheres. Proc. Phys. Soc. 1945; 57: 259-270.

Davies C N. Aerosol Science. London: Academic Press Inc., 1977.

Hanna S R, Briggs G A, Hosker Jr. R P. Handbook on atmospheric diffusion. U.S.Department of Energy, Technical Information Center, 1982.

Hinds W C. Aerosol Technology. New York: John Wiley & Sons, 1982: 38-68.

International Commission on Radiological Protection. 1990 Recommendations of the International Commission on Radiological Protection. ICRP Publication 60. Oxford: Pergamon Press, 1990.

Irwin J S. A theoretical variation of the wind profile law exponent as a function of surface roughness and stability. Atmos. Environ. 1979; 13: 191-194.

Joffre S M. Turbulence and diffusion. University of Helsinki, department of Meteorology, 1983.

Kyle T G. Atmospheric Transmission, Emission and Scattering. First edition, Great Britain, Pergamon Press 1991: 30-32.

Mamuro T, Yoshikawa K, Maki N. Radionuclide fractionation in fallout particles. Health Phys. 1965a; 11: 199-209.

Mamuro T, Fujita A, Matsunami T. Microscope examination of highly radioactive fallout particles from the first Chinese nuclear test explosion. Health Phys. 1965b; 11: 1097-1101.

Mandjukov I G, Mandjukova B V, Alexiev A, Andreev Ts. High activity hot particles in Kozloduy nuclear power plant - status of the investigations. Rad. Prot. Dosim. 1994; 54: 133-138.

National Council on Radiation Protection and Measurements. Limit for Exposure to 'Hot Particles' on the Skin. NCRP Report No. 106. Bethesda, MD:NCRP Publications, 1989.

Nordlund G, Partanen J P, Rossi J, Savolainen I and Valkama I. Radiation doses due to long-range transport of airborne radionuclides released by a reactor accident - effects of changing dispersion conditions during transport. Health Phys. 1985; 49: 1239-1249.

Osuch S, Dąbrowska M, Jaracz P, Kaczanowski J, Le Van Khoi, Mirowski S, Piasecki E, Szeflińska G, Szeflíński Z, Tropiło J, Wilhelmi Z, Jastrzębski J and Pieńkowski L. Isotopic composition of high-activity particles released in the Chernobyl accident. Health Phys. 1989; 39: 707-716.

Pasquill F. The estimation of the dispersion of windborne material. Met. Mag. 1961; 90: 33 - 49.

Pöllänen R, Toivonen H. Skin doses from large uranium fuel particles: application to the Chernobyl accident. Rad. Prot. Dos 1994a; 54: 127-132.

Pöllänen R, Toivonen H. Transport of large uranium fuel particles released from a nuclear power plant in a severe accident. J.Radiol.Prot. 1994b; 14: 55-65.

Pöllänen R, Salonoja M, Toivonen H, Valkama I. Uranium fuel particles in a RBMK accident: particle characteristics and atmospheric dispersion. In: Proceedings of the fifth Finnish national aerosol symposium, June 1-3, 1993. Report series in aerosol science, 1993; N:o 23: 278 - 283

Rogers R R, Yau M K. A Short Course in Cloud Physics. 3rd edition, Great Britain, Pergamon Press 1991: 99-105.

Salbu B, Krekling T, Oughton D H, Østby G, Kashparov V A, Brand T L, Day J P. Hot particles in accidental releases from Chernobyl and Windscale nuclear installations. Analyst 1994; 119: 125-130.

Sandalls F J, Segal M G, Victorova N. Hot particles from Chernobyl: a review. J. Environ. Radioactivity 1993; 18: 5-22.

Sisefsky J. Debris from Tests of Nuclear Weapons. Science 1961; 133: 735-740.

Toivonen H, Pöllänen R, Leppänen A, Klemola S, Lahtinen J, Servomaa K, Savolainen A L, Valkama I. A nuclear incident at a power plant in Sosnovyy Bor, Russia. Health Phys. 1992; 63: 571-573.

Underwood B Y. Gravitational settling of particles dispersing from an elevated point source in the neutral surface layer of the atmosphere. United Kingdom Atomic Energy Authority, Safety and Reliability Directorate, SRD R 516, 1990: 12-15.

United Nations Scientific Committee on the Effects of Atomic Radiation (UNSCEAR). Sources and effects of ionizing radiation. 1993 Report to the general assembly, with scientific annexes. New York: United Nations, 1993. Annex B, table 33: 165-169.

Valkama I, Salonoja M. Operatiiviseen käyttöön soveltuva radioaktiivisten aineiden kaukokulkeutumismalli. Ilmatieteen laitos, Ilmanlaatuosasto, Helsinki, 1993.

Van der Hoven I. In: **Slade D** (ed.) Meteorology and Atomic Energy 1968. Oak Ridge: U.S.Atomic Energy Commission, Office of Information Services, 1968: 202-208.

ACKNOWLEDGEMENTS

We thank Mr Ilkka Valkama, the Finnish Meteorological Institute, for his valuable remarks.

STUK-A reports

STUK-A124 Arvela H. Residential radon in Finland: Sources, variation, modelling and dose comparisons. Helsinki 1995.

STUK-A123 Aaltonen H, Laaksonen J, Lahtinen J, Mustonen R, Rantavaara A, Reponen H, Rytömaa T, Suomela M, Toivonen H, Varjoranta T. Ydinuhkat ja varautuminen. Helsinki 1995.

STUK-A122 Rantavaara A, Saxén R, Puhakainen M, Hatva T, Ahosilta P, Tenhunen J. Radioaktiivisen laskeuman vaikutukset vesihuoltoon. Helsinki 1995.

STUK-A121 Ikäheimonen TK, Klemola S, Ilus E, Sjöblom K-L. Monitoring of radionuclides in the vicinities of Finnish nuclear power plants in 1991-1992. Helsinki 1995.

STUK-A120 Puranen L, Jokela K, Hietanen M. Altistumismittaukset suurtaajuuskuumentimien hajasäteilykentässä. Helsinki 1995.

STUK-A119 Voutilainen A, Mäkeläinen I. Huoneilman radonmittaukset Itä-Uudenmaan alueella: Tilannekatsaus ja radonennuste. Askola, Lapinjärvi, Liljendal, Loviisa, Myrskylä, Mäntsälä, Pernaja, Pornainen, Porvoo, Porvoon mlk, Pukkila, Ruotsinpyhtää ja Sipoo. Helsinki 1995.

STUK-A118 Reiman L. Expert judgment in analysis of human and organizational behaviour in nuclear power plants. Helsinki 1994.

STUK-A117 Auvinen A, Castrén O, Hyvönen H, Komppa T, Mustonen R, Paile W, Rytömaa T, Salomaa S, Servomaa A, Servomaa K, Suomela M. Säteilyn lähteet ja vaikutukset. Helsinki 1994.

STUK-A116 Säteilyturvakeskuksen tutkimushankkeet 1994-1995. Mustonen R, Koponen H (toim.). Helsinki 1994.

STUK-A115 Leszczynski K. Assessment and comparison of methods for solar ultraviolet radiation measurements. Helsinki 1995.

STUK-A114 Arvela H, Castrén O. Asuntojen radonkorjauksen kustannukset Suomessa. Helsinki 1994.

STUK-A113 Lahtinen J, Toivonen H, Pöllänen R, Nordlund G. A hypothetical severe reactor accident in Sosnovyy Bor, Russia: Short-term radiological consequences in southern Finland. Helsinki 1993.

STUK-A112 Ilus E, Puhakainen M, Saxén R. Gamma-emitting radionuclides in the bottom sediments of some Finnish lakes. Helsinki 1993.

STUK-A111 Huurto L, Jokela K, Servomaa A. Magneettikuvauslaitteet, niiden käyttö ja turvallisuus Suomessa. Helsinki 1993.

STUK-A110 Jokela K. Broadband electric and magnetic fields emitted by pulsed microwave sources. Helsinki 1994.

STUK-A109 Saxén R, Aaltonen H, Ikäheimonen TK. Airborne and deposited radionuclides in Finland in 1988-1990. Supplement 11 to Annual Report 1989. Helsinki 1994.

STUK-A108 Arvela H, Mäkeläinen I, Castrén O. Otantatutkimus asuntojen radonista Suomessa. Helsinki 1993.

STUK-A107 Karppinen J, Parviainen T. Säteilyaltistus sydänangiografiatutkimuksissa ja kineangiografialaitteiden toimintakunto. Helsinki 1993.

STUK-A106 Servomaa A, Komppa T, Servomaa K. Syöpäriski säteilyhaittana. Helsinki 1992.

STUK-A105 Mustonen R. Building materials as sources of indoor exposure to ionizing radiation. Helsinki 1992.

STUK-A104 Toivonen H, Klemola S, Lahtinen J, Leppänen A, Pöllänen R, Kansanaho A, Savolainen A.L., Sarkanen A, Valkama I, Jäntti M. Radioactive Release from Sosnovyy Bor, St. Petersburg, in March 1992. Helsinki 1992.

STUK-A103 Ilus E, Sjöblom K-L, Ikäheimonen T.K, Saxén R, Klemola S. Monitoring of radionuclides in the Baltic Sea in 1989-1990. Helsinki 1993.

STUK-A102 Ilus E, Sjöblom K-L, Klemola S, Arvela H. Monitoring of radionuclides in the environs of Finnish nuclear power plants in 1989-1990. Helsinki 1992.

STUK-A101 Toivonen M. Improved processes in therapy dosimetry with solid LiF thermoluminescent detectors. Helsinki 1991.

STUK-A100 Servomaa K. Biological effects of radiation: The induction of malignant transformation and programmed cell death. Helsinki 1991.

STUK-A99 Ruosteenoja E. Indoor radon and risk of lung cancer: an epidemiological study in Finland. Helsinki 1991.

STUK-A98 Kosunen A, Järvinen H, Vatnitskij S, Ermakov I, Chervjakov A, Kulmala J, Pitkänen M, Väyrynen T. Väänänen A. Intercomparison of radiotherapy treatment planning systems using calculated and measured dose distributions for external photon and electron beams. Helsinki 1991.

STUK-A97 Levai F, Tikkinen J, Tarvainen M, Arlt R. Feasibility studies of computed tomography in partial defect detection of spent BWR fuel. Helsinki 1990.

The full list of publications is available from

Finnish Centre for Radiation and Nuclear Safety
P.O. BOX 14
FIN-00881 HELSINKI
Finland
Tel. +358 0 759 881

SÄTEILYTURVAKESKUS
Strålsäkerhetscentralen
Finnish Centre for Radiation
and Nuclear Safety

ISBN 951-712-068-0
ISSN 0781-1705

Painatuskeskus Oy
Helsinki 1995

Sold by:
Finnish Centre for Radiation and Nuclear Safety
P.O. Box 14 FIN-00881 Helsinki
Tel. +358 0 759881